Near and Far Field Characteristics of Two in Line Graphene Coated Dielectric Nanowires Excited by Modulated Electron Beam

Dariia O. Herasymova [1,2]
[1] LMNO, Institute of Radio-Physics and Electronics NASU, Kharkiv, Ukraine
[2] IETR, Universite de Rennes 1, Rennes, France
dariia.heras@gmail.com

***Abstract*— The work is dedicated to the analysis of the infrared and terahertz range diffraction radiation of a beam of charged particles passing above two graphene-covered dielectric nanowires. As usual within DR studies, we assume fixed electron beam velocity, apply the separation of variables in the local coordinates and the addition theorem for the cylindrical functions to satisfy wave-scattering boundary-value problem. For the graphene cover, we use the quantum-theory Kubo formalism and the resistive-type boundary conditions. As a result, we transform the diffraction radiation problem into a Fredholm second-kind matrix equation for the expansion coefficients of the scattered field. Due to such treatment the scattering and absorption characteristics and the field patterns can be found with controlled accuracy. In the focus of the study, there are the resonance effects associated with plasmon supermodes of four different classes of symmetry. Our work can be useful in dielectric laser accelerator design.**

***Keywords*—plasmon, nanowire, graphene, antennas, electromagnetics.**

I. Introduction

The term Diffraction Radiation (DR) was coined to address the electromagnetic-wave emission that appears when electron beams flow nearby dielectric or metal objects without crossing their boundaries. In 1953, Smith and Purcell observed visible-light radiation from an electron beam crossing the grooves of a metal grating; this effect obtained their names [1]. Since then DR has been studied by many researchers, see, for example, [2-5]. The main areas of application of DR are in the non-invasive monitoring of the beam position and velocity [6-9]. Therefore, to simplify the task of DR characterization, one can assume that the beam trajectory and velocity are fixed, and the disturbing action of the electromagnetic field on the beam can be neglected. To have this assumption valid, the DR powers of the radiation and absorption losses should remain small in comparison to the power carried by the beam field.

Meanwhile, for the up-to-date novel miniature particle accelerators the inverse situation is more interesting, where the beam velocity is increased. Today, after almost a century of conventional particle accelerators, which have been important in fundamental physics and other applications, large attention is attracted to the co-called dielectric laser accelerator (DLA) [10,11]. DLAs are micrometer-scale dielectric structures excited by external laser light sources. Due to modern nanofabrication techniques, they can be compact, inexpensive and still provide efficient acceleration due to high electric-field gradients [12]. These devices provide acceleration by using the intensive near fields of laser-driven periodic dielectric structures, i.e. gratings. Additionally, they can incorporate

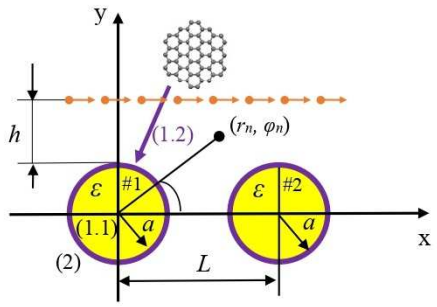

Fig. 1. Cross-sectional geometry of a dimer of identical circular dielectric nanowires with graphene covers and the notations used.

Bragg reflectors to eliminate the incident wave transmission through the grating. A promising material for the DLA is silicon, which has high dielectric permittivity ($\varepsilon \approx 12$) and good thermal conductivity. Besides, its nanofabrication infrastructure is well advanced as examined in [13]. Most popular DLA designs are based on various gratings of circular silicon nanorods [13,14]. They are less expensive and simpler than others and can be mass-produced using available nanofabrication methods. Consequently, electromagnetic analysis of such gratings is interesting and important.

For the DLA designing, it is crucial to have a high electric field gradient near the grating in the beam motion direction. This can be achieved in the natural-mode resonances using the high-index materials like silicon. Still, there is an alternative: plasmon modes supported by the graphene-covered low-index scatterers. Therefore, we chose the research configuration of two dielectric rods covered with graphene shown in Fig. 1.

Due to the fact that graphene sheet maintains low-loss guided plasmon wave in the terahertz and infrared ranges, the electromagnetic properties of such material are close to noble metals, but at much lower frequencies [15]. The exceptionality of graphene is the opportunity to change its conductivity by varying the graphene's chemical potential by means of DC bias [15-17]. Usually, flat dielectric substrates are used for graphene configurations [17-19], however, the curved substrates attract more attention as well [20,21]. Graphene cylindrical nanostructures have been recently investigated in terms of nanospectroscopy measurements [22]. The dimer configuration of circular graphene covered nanowires was studied with the aid of commercial codes in the context of field forces [23] and cloaking [24], and with in-house codes based on the local Fourier expansions in the analysis of eigenfrequencies [25,26].

Besides, such structure was discussed as a model of optical range DR beam position monitor [27].

The aim of our work is the analysis of resonance effects in DR from the same configuration as in [27], however, with two nanowires placed in line along the beam trajectory that is closer to the DLA-related applications than to beam-position ones.

II. Problem Formulation and Basic Equations

Fig. 1 presents the considered geometry of the DR problem. The configuration consists of two identical dielectric nanowires with relative permittivity ε, radius a, and the distance between their axes L. The harmonically modulated, in density, beam of electrons flows at the distance h from the nanorods with the relative velocity $v = \beta c$ ($\beta < 1$). In Fig. 1, we explain the Cartesian and the local (r,φ) polar coordinates used in the derivations. The charge density of the beam as a sheet current flowing along the straight trajectory (in parallel to the x-axis) is assumed modulated with the cyclic frequency ω and given by the function

$$\rho = \rho_0 \delta(y-a-h)\exp[i(kx/\beta - \omega t)], \tag{1}$$

where ρ_0 is an amplitude, $\delta(\cdot)$ is the Dirac delta function and $k = \omega / c$ is the free-space wavenumber. One should note that the harmonically modulated beam charge (1) is connected with the Fourier-transform, in time, of the charge of single particle. In practical terms, the beam charge density can be bunched by external laser radiation or periodic cavity-loaded waveguide.

As known from [2-5], the field of the electron beam (1) is an H-polarized slow surface wave, which propagates along the beam trajectory with the same phase velocity as the beam itself,

$$H_z^0(x,y) = A\beta \,\mathrm{sign}(y-a-h) e^{-q|y-h|} e^{i(k/\beta)x} \tag{2}$$

where $q = k\gamma/\beta$, $\gamma = (1-\beta^2)^{1/2}$ is inverse Lorentz factor, $\mathrm{sign}(\cdot) = \pm 1$, the time dependence is omitted, and the constant in the SI system of units is $A = c\rho_0/2$.

If we consider that the beam velocity is constant, then the DR analysis is reduced to the classical 2-D wave-scattering boundary-value problem, with (2) as the incident field. It includes the Helmholtz equation with the corresponding wavenumbers in partial domains, the graphene boundary conditions at the rod contours, the Sommerfeld radiation condition at infinity, and the condition of the local power finiteness. This set provides uniqueness of problem solution.

We search for the total magnetic field written as follows:

$$H^{tot} = \begin{cases} H^{int(p)}, & r_p < a_p, \quad p = 1,2 \\ H_z^0 + H^{ext}, & r : \{r_p > a_p,\ p = 1,2\} \end{cases} \tag{3}$$

The field in domains (1.1) and (1.2) can be presented as

$$H^{int(p)}(r,\varphi) = \sum_{n=-\infty}^{\infty} y_n^{(p)} J_n(k\alpha r_p) e^{in\varphi_p}, \ r_p < a, \ p = 1,2 \tag{4}$$

$$H^{ext}(r,\varphi) = \sum_{p=1,2} \sum_{n=-\infty}^{\infty} z_n^{(p)} H_n^{(1)}(kr_p) e^{in\varphi_p}, \ r_p > a \tag{5}$$

where $y_n^{(p)}$, $z_n^{(p)}$ are unknown coefficients, $H_m(\cdot)$ and $J_m(\cdot)$ are the first-kind Hankel and the Bessel functions, respectively. The resistive boundary conditions at the nanowire contours, $r_p = a$, $0 \le \varphi_p < 2\pi$, are

$$E_{\varphi_p}^{int(p)}(a,\varphi_p) = E_{\varphi_p}^{0}(a,\varphi_p) + E_{\varphi_p}^{ext}(a,\varphi_p) \tag{6}$$

$$E_{\varphi_p}^{int(p)}(a,\varphi_p) + E_{\varphi_p}^{0}(a,\varphi_p) + E_{\varphi_p}^{ext}(a,\varphi_p) = 2ZZ_0\left[H^{int(p)}(a,\varphi_p) - H^{0}(a,\varphi_p) - H^{ext}(a,\varphi_p)\right] \tag{7}$$

where, $p = 1,2$, $Z_0 = \sqrt{\mu_0/\varepsilon_0}$ is the free space impedance, and the complex-valued relative (i.e. dimensionless, normalized by Z_0) surface impedance of graphene is [15],

$$Z(\omega) = Z_0^{-1}\left(\sigma_{\text{intra}} + \sigma_{\text{inter}}\right)^{-1}, \tag{8}$$

where

$$\sigma_{\text{intra}} = \frac{Z_0\Omega}{1/\tau - i\omega}, \ \sigma_{\text{inter}} = \frac{iq_e^2}{4\pi\hbar}\ln\frac{2|\mu_c| - \left(\omega + i\tau^{-1}\right)\hbar}{2|\mu_c| + \left(\omega + i\tau^{-1}\right)\hbar}, \tag{9}$$

$$\Omega = \frac{q_e^2 k_B T}{\pi\hbar^2 Z_0}\left\{\frac{\mu_c}{k_B T} + 2\ln\left[1 + \exp\left(-\frac{\mu_c}{k_B T}\right)\right]\right\} \tag{10}$$

and τ is the electron relaxation time, q_e is the electron charge, T is the temperature, k_B is the Boltzman constant, $\hbar$ is the reduced Planck constant, and μ_c is the chemical potential. At the frequencies lower than certain μ_c-dependent value, which lays in the near infrared or even visible-light range, $|\sigma_{\text{intra}}| \gg |\sigma_{\text{inter}}|$.

On using (6) and (7) in the series (4) and (5) and a similar series for the field (2), applying Graf's theorem, and introducing new scaled unknowns, $x_n^{(p)} = z_n^{(p)} w_n$ (see [26-28]), where $w_{n<0} = (-1)^n w_{n>0}$, $w_{n>0} = n!(2/ka)^n$, we derive two coupled Fredholm 2-nd kind matrix equations ($p \ne j$ =1,2),

$$x_m^{(p)} \pm w_m^{-1} D_m^{-1} V_m \sum_{n=-\infty}^{+\infty} w_n H_{m-n}(kL) x_n^{(j)} = w_m^{-1} D_m^{-1} F_m^{(p)}, \tag{11}$$

$$V_m = J_m' - iZ\left[J_m' \frac{\alpha J_m(k\alpha a)}{J_m'(k\alpha a)} - J_m\right], \tag{12}$$

$$D_m = H_m' - iZ\left[H_m' \frac{\alpha J_m(k\alpha a)}{J_m'(k\alpha a)} - H_m\right], \tag{13}$$

$$F_m^{(p)} = -g'^{(p)}_m + iZ\left[g'^{(p)}_m \frac{\alpha J_m(k\alpha a)}{J_m'(k\alpha a)} - g_m^{(p)}\right], \tag{14}$$

$$g_m^{(1,2)} = -Ae^{ikL(1\mp 1)/2\beta} e^{-q(a+h)} i^m J_m (1-\gamma)^m \beta^{-m+1}, \tag{15}$$

Here, we have omitted the cylindrical function arguments if they were ka. We would like to stress that the scaling of the

unknowns made above is crucially important for the convergence of the numerical code based on (11) [27].

At $r \to \infty$, we express the scattered field, i.e. the DR field, as $H^{sc}(r,\varphi) = (2/i\pi kr)^{1/2}\Phi(\varphi)\exp(ikr)$, where the angular scattering pattern is a function of $z_m^{(1,2)}$,

$$\Phi(\varphi) = \sum_{m=-\infty}^{+\infty} (-i)^m J_m \left[e^{-\frac{1}{2}ikL\sin\varphi} z_m^{(1)} + e^{\frac{1}{2}ikL\sin\varphi} z_m^{(2)} \right] e^{im\varphi}, \quad (16)$$

Consequently, partial scattering cross-sections (SCS) to the upper and lower half-spaces, respectively, are

$$\sigma_{sc}^{(1,2)} = \frac{2}{\pi k A^2} \int_0^{\pm\pi} |\Phi(\varphi)|^2 d\varphi, \quad (17)$$

Although the dielectric rods can be assumed as lossless, the graphene covers are sizably lossy. Then, the absorption cross sections (ACS) should be introduced, for each nanowire,

$$\sigma_{abs}^{(1,2)} = \pi a \frac{\mathrm{Re}\, Z}{A^2 |Z|^2} \sum_{n=-\infty}^{\infty} \left| A_n^{(1,2)} \right|^2 \quad (18)$$

$$A_n^{(1,2)} = g_n'^{(1,2)} + z_n^{(1,2)} H_n' + J_n' \sum_{m=-\infty}^{\infty} (\pm i)^{m-n} z_m^{(2,1)} H_{n-m}(kL), \quad (19)$$

Similarly to the plane-wave scattering, the sum of all four partial SCS and ACS is the extinction cross-section, σ_{ext}. Then, the Optical Theorem adapted to the DR effect of a modulated beam of electrons can be derived – see [27,28]. Verification of the fulfillment of Optical Theorem numerically can serve as a partial validity check of the obtained results. In our calculations, it has been always fulfilled with machine precision. Comparison of our code results with commercial-code simulations can be found in Fig. 2 of [28].

III. Numerical Results

The scattering and absorption cross sections spectra in the infrared range for two distances between the nanorods are pictured in Fig. 2a. They show a number of the natural-mode resonances. Here, the dimer modes are conveniently called 'supermodes' as they are built on the modes of each circular graphene-covered rod, coupled in one of the four possible ways in the sense of symmetry or anti-symmetry. These quartets form two doublets of closely spaced supermodes [26].

The presence of supermode quartets is revealed in Fig 2b, where the resonances decompose to four peaks, well visible on the zooms of ACS plots around the frequencies of the dipole supermodes P_1. In contrast, in Fig. 2c, where similar zooms around the frequencies of the quadrupole supermodes P_2 are shown, a split of the resonance peaks inside the doublets is not visible. This is caused by the smaller frequency separation of the P_2 supermodes in each doublet.

As one can see, the change of the distance between rods shifts the resonance frequencies. The larger the L, the closer

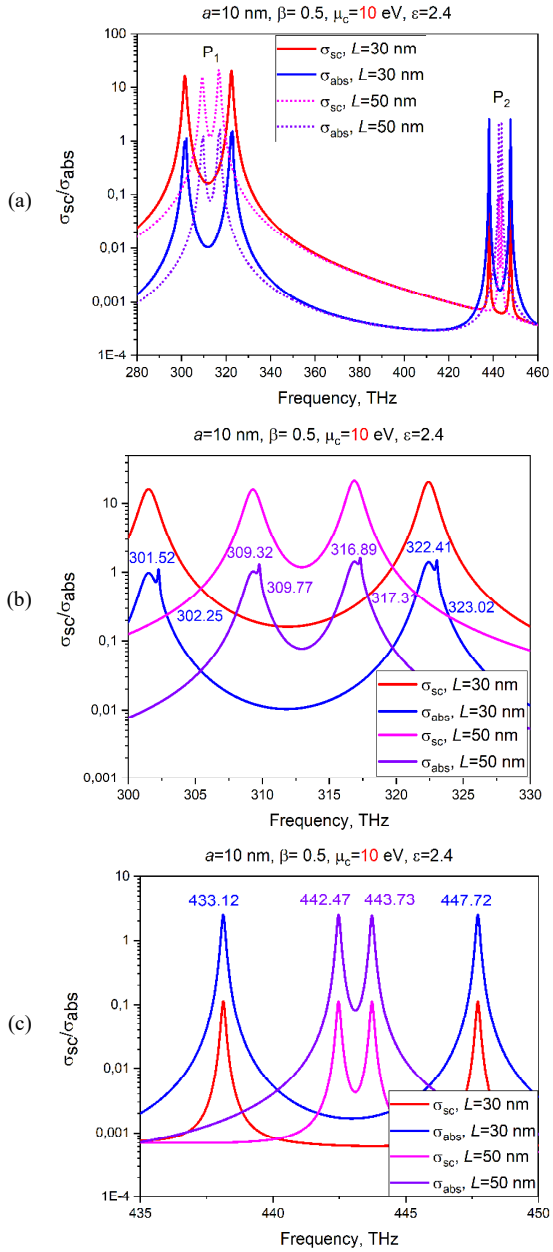

Fig. 2. The spectra of total SCS and ACS of considered model (a) and their zooms around the P_1 (b) and P_2 (c) supermodes. The wire radius is 10 nm, the beam velocity β is 0.5, the beam distance is 5 nm, the chemical potential is 10 eV, the electron relaxation time is 1 ps, the temperature is 300 K, the dielectric permittivity is 2.4, and the distance between the wire axes is 30 nm and 50 nm.

the frequencies of all peaks to the frequency of the plasmon mode of the single circular rod covered with graphene [26].

In order to visualize the symmetry classes of the resonating supermodes, we present the near magnetic field patterns and the far field angular patterns of the supermodes P_2, see Fig. 3.

One can see different orientation of the field maxima (red spots) that corresponds to different supermode symmetry classes. Each wire displays four bright spots of the field maxima. Here, only two of the possible four symmetry orientations appear due to unresolved resonances of the P_2 peaks.

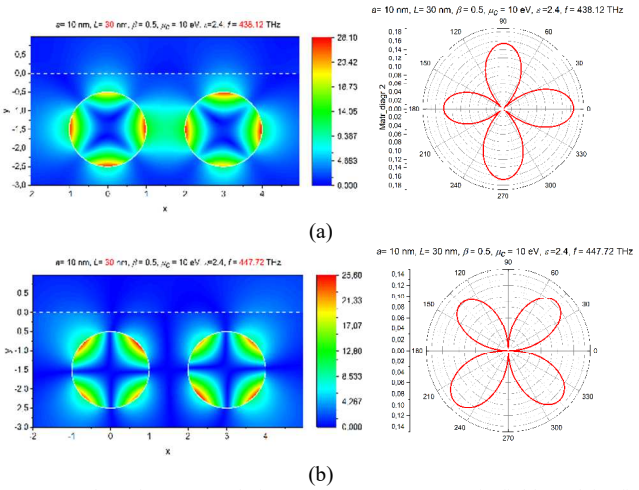

(a)

(b)

Fig. 3. Quadrupole supermode in-resonance near magnetic fields and far field patterns of graphene-covered wire dimer. The wire and beam parameters are the same as in Fig. 4, and the distance between the wires is 30 nm.

Their Q-factors are not large enough to distinguish all symmetry classes. For the panel (a), the resonance is on the *x*-even/*y*-even P_2 supermode at the frequency of 433.12 THz. For the panel (b), the resonance is on the *x*-odd/*y*-odd P_2 supermode at 447.72 THz. Note that in-resonance field magnitude maxima are around 25 times larger than the magnetic-field maximum for the same beam in the free space. This enhancement can be exploited in DLA design. However, the field high values decay quickly off the rod boundaries as typical for the plasmon modes. The rate of decay is close to exponential near the boundary, however, transforms to $r^{-1/2}$ in the far zone.

IV. Conclusions

We have presented basic equations and sample numerical results for the diffraction radiation from two in-line dielectric circular nanorods with graphene covers exited by the modulated electron beam. The resonances on the plasmon supermodes of different symmetries have been discussed. This analysis can be useful in the design of DLA sections made of low-index dielectrics, however, covered with graphene.

Acknowledgments

This work was partially funded by NASU via project #2022-0204-6541230. Besides, support of the Program PAUSE – Solidarity with Ukraine of the Ministry of Higher Education, Research and Innovations, France and hospitality of the IETR, Universite de Rennes are acknowledged with gratitude.

References

[1] S. J. Smith and E. M. Purcell, “Visible light from localized surface charges moving across a grating,” Phys. Rev., vol. 92, art. no 1069, 1953.

[2] A. I. Nosich, "Diffraction radiation which accompanies the motion of charged particles near an open resonator," Radiophys. Quant. Electron., vol. 24, no 8, pp. 696-701, 1981.

[3] L. A. Pazynin and V. G. Sologub, “Radiation of a point charge moving uniformly along the axis of a narrow cylindrical ring,” Radiophys. Quant. Electron., vol. 25, no 1, pp. 64-68, 1982.

[4] A. I. Boltonosov and V. G. Sologub, "Excitation of an open strip-type resonator by a modulated beam of charged particles," Sov. J. Communic. Technol. Electron., vol. 33, no 6, pp. 133-140, 1988.

[5] G. I. Zaginaylov, et al., "Modeling of plasma effect on the diffraction radiation of relativistic beam moving over a grating of finite extent," Microwave Opt. Technol. Lett., 16, no 1, pp. 50-54, 1997.

[6] M. Castellano, et al., "Measurements of coherent diffraction radiation and its application for bunch length diagnostics in particle accelerators," Phys. Rev. E, vol. 63, art. no 056501, 2001.

[7] L. Bobb, R. Kieffer, et al., "Feasibility of diffraction radiation for noninvasive beam diagnostics as characterized in a storage ring," Phys. Rev. Accel. Beams, vol. 21, art. no 03801, 2018.

[8] M. Bergamaschi, et al., “Noninvasive micrometer-scale particle-beam size measurement using optical diffraction radiation in the ultraviolet wavelength range,” Phys. Rev. Appl., vol. 13, no 1, pp. 014041, 2020.

[9] D. Assante, et al., “Longitudinal coupling impedance of a particle traveling in PEC rings: A regularised analysis,” IET Microwaves Antennas Propagat., vol. 35, no 10, pp. 1318–1329, 2021.

[10] R. J. England et.al., “Dielectric laser accelerators,” Rev. Mod. Phys., vol 86, no 4, pp. 1337-1389, 2014.

[11] Y. Wei, et al., "Dual-grating dielectric accelerators driven by a pulse-front-tilted laser," Appl. Opt., vol. 56, pp. 8201-8206, 2017.

[12] J. Breuer et al., “Laser-based acceleration of nonrelativistic electrons at a dielectric structure,” Phys. Rev. Lett., 111, 134803, 2013.

[13] K. J. Leedle et.al., “Phase-dependent laser acceleration of electrons with symmetrically driven silicon dual pillar gratings,” Opt. Lett., vol. 43, pp. 2181-2184, 2018.

[14] R. Shiloh, T. Chlouba, P. Yousefi, and P. Hommelhoff, “Particle acceleration using top-illuminated nano-photonic dielectric structures,” Opt. Exp., vol. 29, no 10, pp. 14403-14411, 2021.

[15] G. W. Hanson, “Dyadic Green’s functions and guided surface waves for a surface conductivity model of graphene,” J. Appl. Phys., vol. 103, art. no 064302, 2008.

[16] T. Low and P. Avouris, “Graphene plasmonics for terahertz to mid-infrared applications,” ACS Nano vol. 8, pp. 1086–1101, 2014.

[17] Z. Ullah, et al., “A review on the development of tunable graphene nanoantennas for terahertz optoelectronic and plasmonic applications,” Sensors, vol. 20, no 5, art. no 1401, 2020.

[18] F. O. Yevtushenko, et al., “Spoiling of tunability of on-substrate graphene strip grating due to lattice-mode-induced transparency,” RSC Advances, vol. 12, no 8, pp. 4589–4594, 2022.

[19] M. Lucido, M. V. Balaban, and A. I. Nosich, “Terahertz range plasmon and whispering gallery mode resonances in the plane wave scattering from thin microsize dielectric disk with graphene covers,” Proc. Royal Society A, vol. 478, no 2262, art. no 20220126, 2022.

[20] J. Zhao, et al., "Surface-plasmon-polariton whispering-gallery mode analysis of the graphene monolayer coated InGaAs nanowire cavity," Opt. Exp. vol. 22, pp. 5754-5761, 2014.

[21] J. P. Liu, X. Zhai, L. L. Wang, H.-J. Li, F. Xie, Q. Lin, and S.-X. Xia, “Analysis of mid-infrared surface plasmon modes in a graphene-based cylindrical hybrid waveguide,” Plasmonics, vol. 11, pp. 703–711, 2016.

[22] C. Dai, et al., “Hybridized radial and edge coupled 3D plasmon modes in self-assembled graphene nanocylinders,” Small, vol. 17, art. no 2100079, 2021.

[23] B. Zhu, et al., "Field enhancement and gradient force in the graphene-coated nanowire pairs," Plasmonics, vol. 10, no 4, pp. 839-845, 2015.

[24] M. Naserpour, et al., "Tunable invisibility cloaking by using isolated graphene-coated nanowires and dimers," Sci. Rep., vol. 7, pp. 1-14, 2017.

[25] M. Cuevas, S. H. Raad, and C. J. Zapata-Rodríguez. "Coupled plasmonic graphene wires: theoretical study including complex frequencies and field distributions of bright and dark surface plasmons," J. Opt. Soc. Am. B, vol. 37, no10, pp. 3084-3093, 2020.

[26] D. O. Herasymova, et al., “Threshold conditions for transversal modes of tunable plasmonic nanolasers shaped as single and twin graphene-covered circular quantum wires,” IOP Nanotechnology, vol. 33, no 49, art. no 495001, 2022.

[27] D. O. Herasymova, S. V. Dukhopelnykov, and A. I. Nosich, “Infrared diffraction radiation from twin circular dielectric rods covered with graphene: plasmon resonances and beam position sensing,” J. Opt. Soc. Am. B, vol. 38, no 9, pp. C183-C190, 2021.

[28] D.O. Herasymova, et al, “Optical sensing of electron-beam position with twin silver nanotube antenna tuned to hybrid surface plasmon resonance,” IEEE J. Sel. Top. Quant. Electron., vol. 27, no 1, art. no 4601008, 2021.